JOURNAL OF VIROLOGY, Sept. 1995, p. 5269–5277 Vol. 69, No. 9
0022-538X/95/$04.00+0

Membrane Protein Molecules of Transmissible Gastroenteritis Coronavirus Also Expose the Carboxy-Terminal Region on the External Surface of the Virion

CRISTINA RISCO,[1] INÉS M. ANTÓN,[1] CARLOS SUÑÉ,[1] ANA M. PEDREGOSA,[1]†
J. MANUEL MARTÍN-ALONSO,[2] FRANCISCO PARRA,[2]
JOSÉ L. CARRASCOSA,[1] AND LUIS ENJUANES[1]*

Centro Nacional de Biotecnología, Consejo Superior de Investigaciones Científicas, Campus Universidad Autónoma, Cantoblanco, 28049 Madrid,[1] and Departamento de Biología Funcional, Facultad de Medicina, Universidad de Oviedo, 33006 Oviedo,[2] Spain

Received 13 February 1995/Accepted 22 May 1995

The binding domains of four monoclonal antibodies (MAbs) specific for the M protein of the PUR46-MAD strain of transmissible gastroenteritis coronavirus (TGEV) have been located in the 46 carboxy-terminal amino acids of the protein by studying the binding of MAbs to recombinant M protein fragments. Immunoelectron microscopy using these MAbs demonstrated that in a significant proportion of the M protein molecules, the carboxy terminus is exposed on the external surface both in purified viruses and in nascent TGEV virions that recently exited infected swine testis cells. The same MAbs specifically neutralized the infectivity of the PUR46-MAD strain, indicating that the C-terminal domain of M protein is exposed on infectious viruses. This topology of TGEV M protein probably coexists with the structure currently described for the M protein of coronaviruses, which consists of an exposed amino terminus and an intravirion carboxy-terminal domain. The presence of a detectable number of M protein molecules with their carboxy termini exposed on the surface of the virion has relevance for viral function, since it has been shown that the carboxy terminus of M protein is immunodominant and that antibodies specific for this domain both neutralize TGEV and mediate the complement-dependent lysis of TGEV-infected cells.

Transmissible gastroenteritis coronavirus (TGEV) causes enteric disease in swine of all ages. The disease is specially severe in newborn animals less than 2 weeks old, in which mortality approaches 100% (36). Four structural proteins have been described for TGEV: spike protein (S), nucleoprotein (N), membrane protein (M), and a recently identified small membrane protein (sM), with 1,447, 382, 262, and 78 amino acids, respectively (11, 12, 15, 16, 27). S protein, which has characteristics similar to those of spike proteins from other viruses, is the major inducer of virus-neutralizing antibodies (7, 8, 11, 14, 27). M protein, however, differs markedly from other viral proteins in structure, processing, and intracellular transport (39). M protein induces antibody-dependent complement-mediated virus neutralization (8, 44). Although its function is unclear, M protein is required for virus assembly and budding, in contrast to S protein, which is not essential for these activities, as reported for mouse hepatitis virus (MHV) (32, 39, 40, 43).

The nucleotide sequence predicted for the TGEV M protein shares many features with the M proteins of MHV, bovine coronavirus, and avian infectious bronchitis virus but is distinctive in that it predicts a potentially cleavable amino-terminal signal peptide for membrane insertion (16, 21). Moreover, the amino terminus of TGEV M protein extends 54 amino acids from the virion envelope, compared with only 28 for bovine coronavirus, 26 for MHV, and 21 for avian infectious bronchitis virus (2, 16, 19).

Theoretical methods applied to the amino acid sequences of both MHV and avian infectious bronchitis virus M protein (1, 33) as well as limited proteolysis and immunolabeling assays of the MHV-A59 M protein assembled in microsomal and intracellular membranes (23, 24, 31) led to the currently accepted topological model of M protein. According to this model, the protein spans the membrane three times and has a relatively hydrophilic intravirion carboxy-terminal region largely resistant to proteolysis. The model proposes the existence of two different hydrophilic peptides, each projecting on a different side of the membrane (33). For a fine determination of the topology of wild-type and mutant MHV M proteins expressed in MDCK-II cells with vaccinia virus vectors, immunofluorescence experiments using domain-specific antibodies and permeabilized cells revealed a variety of topologies for the mutant proteins assembled in intracellular membranes (24). While some of the mutant M proteins exhibited the wild-type topology, in others, the carboxy terminus was oriented toward the lumen of the endoplasmic reticulum. Furthermore, one of them exhibited two different topologies: some molecules had both the NH_2 and COOH termini oriented toward the lumen of the endoplasmic reticulum, while others had both domains exposed on the cytoplasmic side (23, 24). This could allow for alternative positioning of these domains (24). In the case of TGEV, previous experimental observations have suggested that a portion of the M protein molecules may also exhibit a topology different from that described for wild-type MHV M protein. This hypothesis was based on (i) antibody-mediated complement-dependent cytolysis of TGEV-infected cells, using monoclonal antibodies (MAbs) specific for the M protein carboxy terminus and (ii) detection in immunofluorescence

* Corresponding author. Mailing address: Department of Molecular and Cell Biology, Centro Nacional de Biotecnología, Campus Universidad Autónoma, Cantoblanco, 28049 Madrid, Spain. Phone: (341) 585 4555. Fax: (341) 585 4506. Electronic mail address: LENJUANES@samba.cnb.uam.es.

† Present address: Departamento de Microbiología y Parasitología, Universidad de Alcalá de Henares, 28871 Madrid, Spain.

studies of the carboxy terminus of TGEV M protein exposed on the surface of infected cells (10, 22). The analysis of the topological organization of M protein in the infective viral particle (which has completed the structural transformation associated with intracellular budding and exited the cell) requires the application of a method capable of discriminating at the level of single viruses. Suspensions of purified viruses include intact as well as partially disrupted virions, and limited proteolysis analysis does not discriminate between them. Moreover, degradation patterns cannot be interpreted when two different topologies coexist (24). Topological studies of viral particles can be alternatively done by mapping with domain-specific MAbs, a strategy used by Locker et al. (24) to determine the topology of M proteins assembled in intracellular membranes. Immunoelectron microscopy has been successfully applied for a precise detection of particular protein domains in viral particles (5, 26, 29), and neutralization assays allow a correlation between topological data and functional aspects of the virus (41).

In this study, several MAbs specific for the carboxy terminus of TGEV PUR46 M protein were identified. By immunogold mapping using domain-specific MAbs and electron microscopy, we observed that the carboxy-terminal domain of M protein is accessible to two of these MAbs on the surface of purified TGEV virions and on virions that recently exited the infected cells. In addition, neutralization assays showed that the carboxy terminus of M protein is exposed on infectious viral particles, an observation consistent with the previous finding that this domain is exposed on the surface of TGEV-infected cells.

MATERIALS AND METHODS

Viruses. The PUR46-MAD and MIL65 strains of TGEV (14, 37) were used to infect swine testis (ST) cells (25). The M gene from the FS772/70 strain of TGEV (3) was used to express recombinant fragments of this protein in a prokaryotic system. Cell culture, virus infections, and purifications of TGEV were performed as previously described (7, 14, 41). Suspensions of freshly isolated viruses, with a titer of 10^9 PFU/ml, were maintained at −20°C until use.

Antibodies. The murine MAbs specific for the C terminus of TGEV M protein were previously obtained (14, 37), and their characterization is presented in this report. On the basis of the binding to purified virus strains, the four M-specific MAbs recognized at least two different sets of epitopes: one defined by MAbs 3B.B3, 3B.D3, and 3D.E3, and another one defined by MAb 9D.B4 (37). The MAbs specific for TGEV S protein (6A.C3, 8F.B3, and 1D.G3) and N protein (3D.H10, 3D.C10, and 3B.B6) were obtained and described previously (7, 11, 14, 37). MAb 25.22, specific for the M protein amino terminus (20), was kindly provided by H. Laude (Institut National de la Recherche Agronomique, Jouy-en-Josas, France).

The hyperimmune sera against the PUR46-MAD strain of TGEV were produced in haplotype cc miniswine (35) and mice (14). Serum against the FS772/70 strain of TGEV, which was raised in gnotobiotic piglets, was kindly provided by P. Britton (AFRC Institute for Animal Health, Compton, England). A rabbit anti-mouse immunoglobulin antiserum was purchased from Cappel (Durham, N.C.).

Virus neutralization. Aliquots of 50 μl of the PUR46-MAD strain of TGEV (serial 10-fold dilutions in 0.15 mM phosphate-buffered saline [PBS; pH 7.4], containing 2% fetal calf serum [PBS-FCS]) were incubated 30 min at 37°C with 50 μl of undiluted hybridoma supernatants with the corresponding MAb. Rabbit anti-mouse immunoglobulins (50 μl; diluted 1:20 in PBS-FCS) were added, and the mixtures were incubated for another 30 min. The mixtures were plated on ST monolayers without further dilution, and the residual infectivity was determined as previously described (14).

Cloning and expression of recombinant M protein antigens. M gene fragments were cloned into vectors pUR 290, 291, and 292 as previously described (34), under the control of *lac* operon, using the restriction endonuclease sites shown in Fig. 1, which also shows the M protein residues contained in each construct. Recombinant plasmids were transferred into *Escherichia coli* XL1-Blue cells to produce β-galactosidase fusion proteins. Plasmid DNA was purified, and insertions were checked for correct orientation by restriction analysis (not shown). When convenient, the junction area of the construct was also sequenced.

M structure predictions, made with the programs of the Genetics Computer Group (University of Wisconsin), were calculated for the amino acid sequence of the M protein of TGEV (PUR46 strain). This sequence was predicted from the corresponding nucleotide sequence of the M gene (16, 21). Hydrophilicity, surface exposure probability, and glycosylation profiles of M protein were determined by using the computer programs developed by Devereux et al. (9).

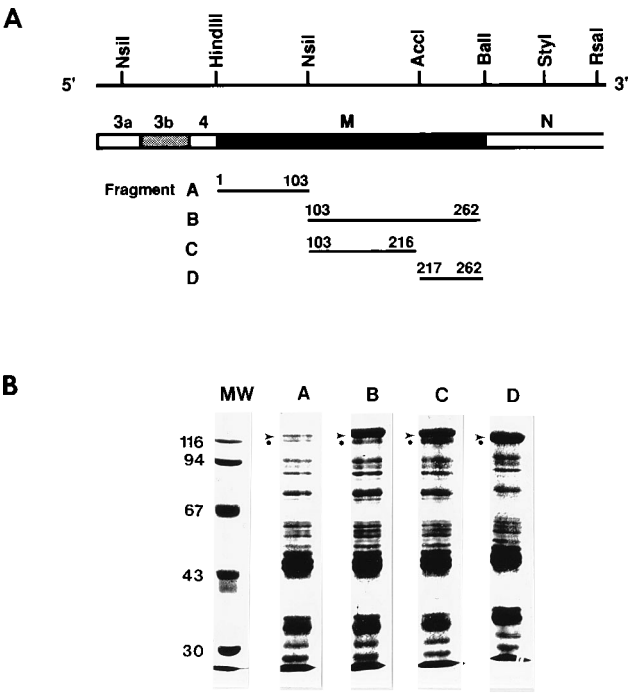

FIG. 1. Strategy used to derive the fusion proteins from the M gene and protein patterns expressed by recombinant bacteria. (A) Four domains of M protein coded by fragments A, B, C, and D of the M gene were expressed as fusion proteins at the β-galactosidase carboxy terminus. Location of amino acids flanking the fragments are indicated above thin lines. The upper line shows key restriction endonuclease activities used to generate these fragments. Boxes show the M gene and open reading frames flanking this gene. (B) SDS-PAGE analysis of the proteins synthesized by *E. coli* XL1-Blue cells transformed with pUR plasmids containing the four M gene inserts indicated in panel A. Proteins were stained with Coomassie blue. Arrowheads point to the recombinant fusion product of the M protein fragment and β-galactosidase; dots indicate the position of β-galactosidase. MW, molecular weight markers (sizes are indicated in kilodaltons).

SDS-PAGE and Western blotting (immunoblotting). Cell extracts of recombinant *E. coli* cultures, induced with 200 mM isopropyl-β-D-thiogalactopyranoside (IPTG) for 2 h at 37°C, were fractionated by polyacrylamide gel electrophoresis in the presence of sodium dodecyl sulfate (SDS-PAGE), using 8% acrylamide gels and conditions described by Laemmli (18). Transfer to nitrocellulose membranes (Millipore HAHY00010; pore size, 0.45 nm) was done as described by Burnette (4) with a Bio-Rad Mini Protean II electroblotting apparatus at 100 V for 1 h in 25 mM Tris–192 mM glycine buffer (pH 8.3) containing 20% methanol. After the transfer, the nitrocellulose membranes were blocked for 1 h at room temperature with PBS (1.5 mM KH_2PO_4, 8.1 mM Na_2HPO_4, 2.7 mM KCl, 140 mM NaCl) containing 1% gelatin and 0.1% Tween 20 (PTG buffer). The membranes were then incubated for 1 h in the appropriate dilution of the corresponding hyperimmune antiserum or the specific MAb and subsequently incubated for 1 h with anti-mouse antibodies (1/2,000 in PTG) and 1 h more with 0.1 mCi of [^{125}I]protein A (Amersham International, Amersham, England) per ml. Swine polyclonal antibodies against TGEV antigens were directly detected with [^{125}I]protein A in PTG buffer.

Immunogold labeling of isolated virions. Localization of different epitopes of S and M proteins exposed on the surface of TGEV particles was done by immunogold labeling and electron microscopy, using MAbs against different epitopes of S, M, and N proteins of TGEV and a goat anti-mouse immunoglobulin G–5-nm colloidal gold conjugate, provided by Biocell Research Laboratory (Cardiff, Wales). Two MAbs, 6A.C3 and 1D.G3, were used to detect A and D antigenic sites of S protein, respectively. To localize the carboxy-terminal region of M protein, four different MAbs, 9D.B4, 3B.B3, 3B.D3, and 3D.E3, were used. The amino-terminal domain of M protein was labeled with MAb 25.22. MAbs 3B.B6, 3D.C10, and 3D.H10, which are specific for the internal nucleocapsid, were used as cytochemical controls for detection of the epitopes exposed on the surface of the virions. For detection of the 9D.B4 site, freshly isolated and fixed viruses were used. Viral suspensions were fixed for 30 min with a solution of 4%

paraformaldehyde and 0.05% glutaraldehyde in 1 mM PBS (pH 7.4) and kept at 4°C until labeling was performed. Immunodetection of TGEV proteins on virions was performed as described previously (5, 26, 29). Viruses were attached to electron microscopy grids covered with Formvar and carbon and previously made hydrophilic by glow discharge. These grids were placed on drops of concentrated TGEV suspensions and incubated for 5 min. After removal of excess liquid by touching the edge of the grid with filter paper, immunolabeling was performed by placing the grids on drops of different solutions. All incubations were done at room temperature. The first step was a 10-min incubation with TBG (30 mM Tris-HCl [pH 8.2] containing 150 mM NaCl, 0.1% bovine serum albumin, and 1% gelatin) to block nonspecific binding of the antibodies to the samples. Grids were then transferred to drops of undiluted MAbs and incubated for 30 min. After being washed by transferring the grids through several drops of TBG, the samples were further incubated for 30 min with a conjugate of goat anti-mouse immunoglobulin G–5-nm colloidal gold (diluted 1:20 in TBG). Grids were then floated on 3 drops of TBG and 3 more drops of distilled water before negative staining for 40 s with a 2% solution of uranyl acetate. Samples were finally examined in a JEOL 1200 EX II electron microscope.

Preembedding immunogold labeling of virus-producing cell cultures. The localization of TGEV protein epitopes exposed on virus-producing cells was performed by immunogold detection on cell cultures at 14 h postinfection. Cultures producing PUR46 or MIL65 TGEV were placed at 4°C before the culture medium was replaced by the corresponding MAb (9D.B4, 6A.C3, 1D.G3, and 3D.H10 for cultures producing PUR46 TGEV and only 9D.B4 for cultures producing MIL65 TGEV). Incubation with the MAbs was maintained for 2 h at 4°C. After the antibodies were removed and the monolayers were washed with PBS-FCS, a 5-nm gold conjugate (goat anti-mouse immunoglobulin G) diluted 1:40 in the same buffer was added to the cultures, which were maintained 1 h at 4°C. After three washes with cold PBS, monolayers were submitted to a mild fixation in situ with a solution of 4% paraformaldehyde and 0.05% glutaraldehyde in PBS for 30 min at 4°C. Fixed cells were then removed from the dishes with a plastic pipette and transferred to Eppendorf tubes. After centrifugation in a microcentrifuge and washing with PBS, the pellets were processed for embedding in Lowicryl K4M at low temperature as previously described (28, 30). Control cultures (noninfected cells) as well as TGEV-producing cells were incubated in the same conditions but in the absence of antibodies and processed for embedding in Lowicryl K4M. Thin sections of the samples were stained for 20 min with a saturated solution of uranyl acetate and studied by electron microscopy.

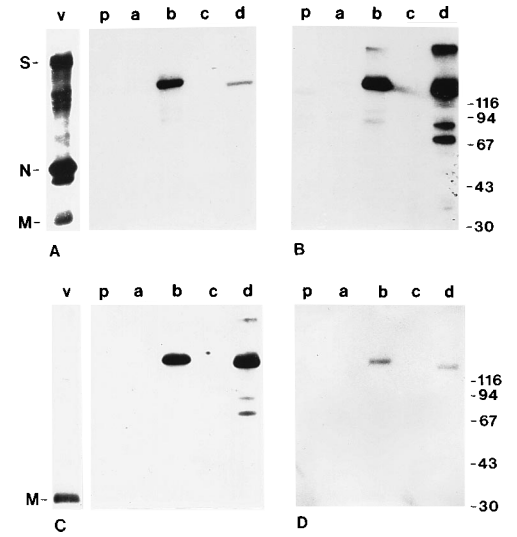

FIG. 2. Western blot analysis of recombinant antigens coded by M gene. (A) Lanes a through d correspond to extracts from cells transformed with plasmids carrying fragments A through D (see Fig. 1) of the integral membrane protein. These extracts were transferred onto nitrocellulose paper and analyzed by Western blotting with a swine antiserum specific for TGEV (FS772/70 strain) (A) or a serum from mice immunized with the PUR46 strain of TGEV (B). Lanes p represent binding to extracts from cells transformed with the plasmid lacking the insert; lane v shows binding to extracts from TGEV-infected ST cells. (C and D) Western blot analysis of the extracts indicated in panel A, developed with two different anti-M protein MAbs, 3B.B3 (C) and 9D.B4 (D). Molecular masses were estimated by comparison with the indicated standards (116, 94, 67, 43, and 30 kDa) and the TGEV structural proteins (220, 47, and 29 kDa for S, N, and M proteins, respectively).

RESULTS

MAb characterization. To determine the antigenicity of M protein and the domains recognized by four M-specific MAbs, their binding to recombinant M fragments coding for different areas of the glycoprotein was studied. Four M protein fragments containing amino acids 1 to 103, 103 to 262, 103 to 216, and 217 to 262 were expressed as fusion proteins with β-galactosidase and named A, B, C, and D, respectively (Fig. 1A). The hybrid proteins were analyzed by SDS-PAGE as described in Materials and Methods. In all cases, recombinant antigens with molecular masses higher than that of β-galactosidase (116 kDa) were detected by Coomassie blue staining (Fig. 1B). The antigenicities of the fusion proteins was determined by studying their binding to swine polyclonal antibodies against the F772/70 strain of TGEV and with serum from mice immunized against the PUR46 strain of TGEV. The results (Fig. 2A and B) showed that fragments B and D were recognized by the porcine and murine sera, indicating that the fragments containing the carboxy terminus were the most immunogenic regions of the membrane protein fused to β-galactosidase and that fragments containing only the amino terminus from M protein were not bound by polyvalent antisera. Both the polyvalent murine antiserum and the MAbs bound to recombinant products of the expected molecular masses (121 and 133 kDa) and, in addition, to molecular products with higher and lower molecular masses which probably correspond to aggregates and degradation products of the fusion protein M–β-galactosidase. In fact, the tendency of M protein to aggregate has been previously observed (6, 40). The additional bands of higher and lower molecular masses most likely do not correspond to nonspecific binding, since they were detected only in the presence of recombinant products containing the M protein carboxy terminus by four MAbs. Extracts from induced cells transformed with pUR vectors without insert or noninduced recombinants did not bind the antiserum.

To define the antigenic domains recognized by M-specific MAbs in the TGEV M protein, their binding to recombinant antigens blotted onto nitrocellulose filters was studied (Fig. 2C and D). All four MAbs (3B.B3, 3B.D3, 3D.E3, and 9D.B4) bound to recombinant fragments B and D but not to fragments A and C or to proteins from cells transformed with pUR plasmids that did not contain the insert. Results for all MAbs were identical, and only recombinant proteins containing the 46 amino acids of the carboxy terminus of M protein were recognized by the four MAbs. Thus, the different epitopes recognized by these MAbs (37) are localized in the last 46 amino acids.

Topology of S and M protein domains in isolated TGEV virions. Isolated TGEV virions exhibit the typical coronavirus morphology of round enveloped particles with surface projections, as visualized by negative staining (Fig. 3A). Immunogold labeling of TGEV proteins on viral particles reveals the epitopes of the envelope proteins exposed on the surface of the virions that are accessible to the MAbs (Fig. 3B to N). Specific detection of S protein was done with 6A.C3 (a MAb specific for the A site of S protein), and labeling was comparable in two related strains, PUR46 (Fig. 3B) and MIL65 (Fig. 3C). A strong labeling was usually observed. It is important to note that the gold marker is always visualized at a certain distance from the localized antigen. This distance relates to the size of the immunocomplexes and varies with the degree of extension during the drying of the sample. When 5-nm gold particles and two immunoglobulin molecules are used, the distance between the gold marker and antigen is about 15 to 25 nm (17). To assess the specificity of the labeling, an immunocytochemical

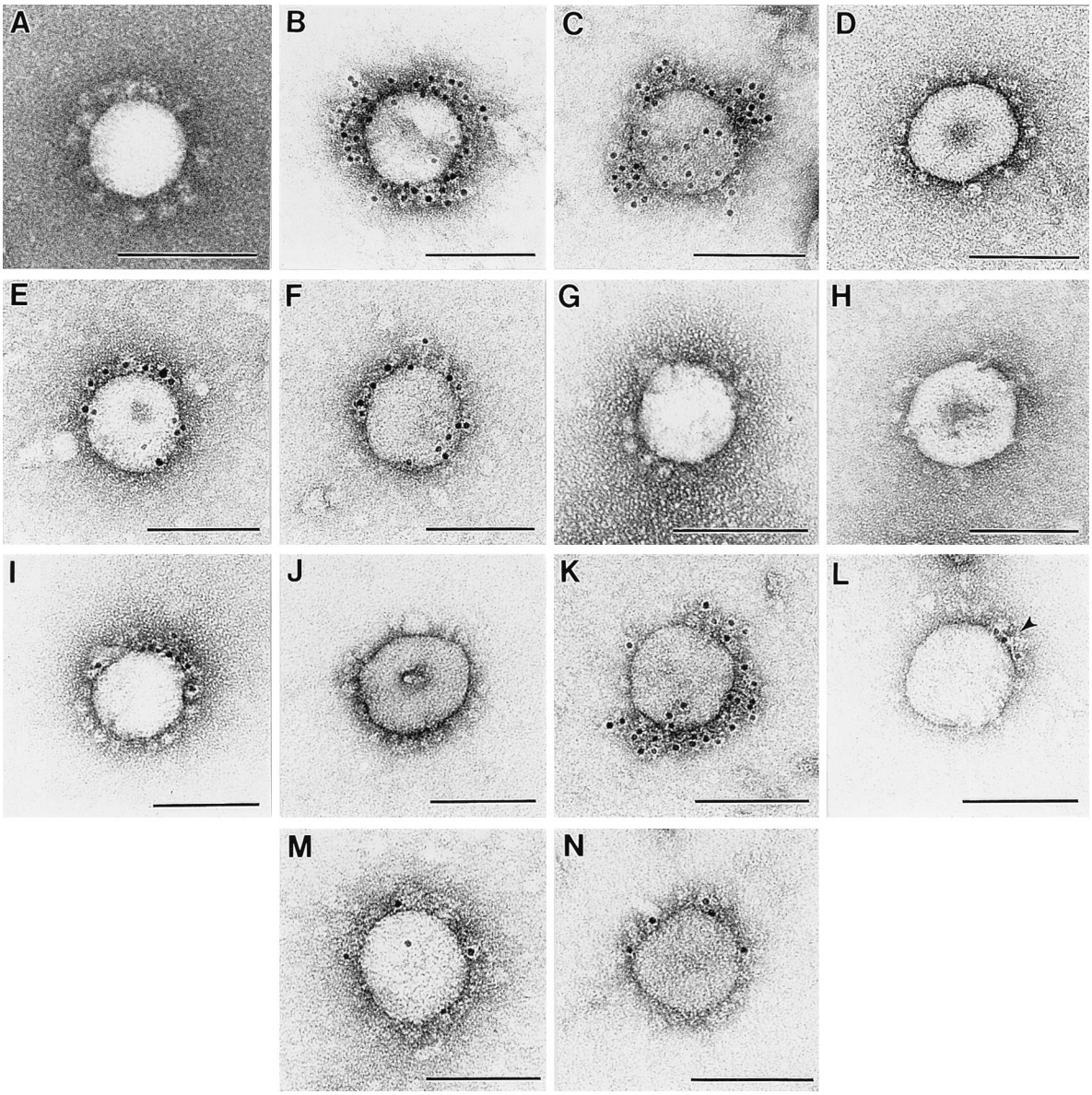

FIG. 3. Immunogold localization of different epitopes of M and S proteins on the surface of TGEV virions, using MAbs and a 5-nm colloidal gold conjugate. (A) General morphology of TGEV by negative staining with 2% sodium phosphotungstate. (B and C) Localization of the A site of S protein with MAb 6A.C3. A heavy reaction is detected in PUR46 (B) and MIL65 (C) virions. (D) No reaction is obtained with 3D.H10, a MAb directed against the internal nucleocapsid protein and that here represents a cytochemical control. (E and F) PUR46 TGEV particles labeled with 9D.B4, a MAb that recognizes an epitope of the carboxy-terminal domain of M protein. (G and H) MAb 9D.B4 does not recognize the surface of MIL65 virions lacking the 9D.B4 site. Fixed PUR46 virions present a weak reaction with MAB 9D.B4 (I), while fixed MIL65 virions do not react with 9D.B4 (J). 3B.B3, a MAb that recognizes a different epitope of the carboxy-terminal domain of M protein, strongly reacts with the surface of PUR46 TGEV virions (K), but labeling is very weak on MIL65 virions (L). MAb 25.22, which recognizes an epitope of the amino-terminal domain of M protein, reacts with the surface of PUR46 (M) and MIL65 virions (N), showing no difference in the level of exposure of this region of the M protein in the two viral strains. Bars, 100 nm.

control assay was done with 3D.H10, a MAb directed against the internal nucleocapsid of TGEV. This MAb does not react with the virions, which also confirms that the viral envelope is impermeable to antibodies against internal antigens (Fig. 3D). As an additional control, a MAb that recognizes the capsid protein of murine leukemia virus was used as a primary antibody. This MAb (6D.2) did not bind to TGEV virions (not shown). In addition, goat anti-mouse antibodies conjugated with colloidal gold did not bind the viruses in the absence of a specific primary MAb. Localization of the M protein was done with several MAbs against the carboxy-terminal region of this protein (Fig. 3E to L) and a MAb specific for the amino-terminal region (Fig. 3M and N). The carboxy-terminal domain is actually exposed on the surface of PUR46 TGEV virions, as revealed by labeling with MAb 9D.B4 (Fig. 3E and F). To rule out nonspecific binding, a key control experiment was performed with the same MAb and a virus strain (MIL65) which does not contain the epitope defined by MAb 9D.B4 (37). This antibody did not bind the MIL65 strain of TGEV (Fig. 3G and H). This decisive control confirms the specificity of the labeling with 9D.B4 in PUR46 TGEV and the exposure of the M protein C terminus on the surface of PUR46 TGEV.

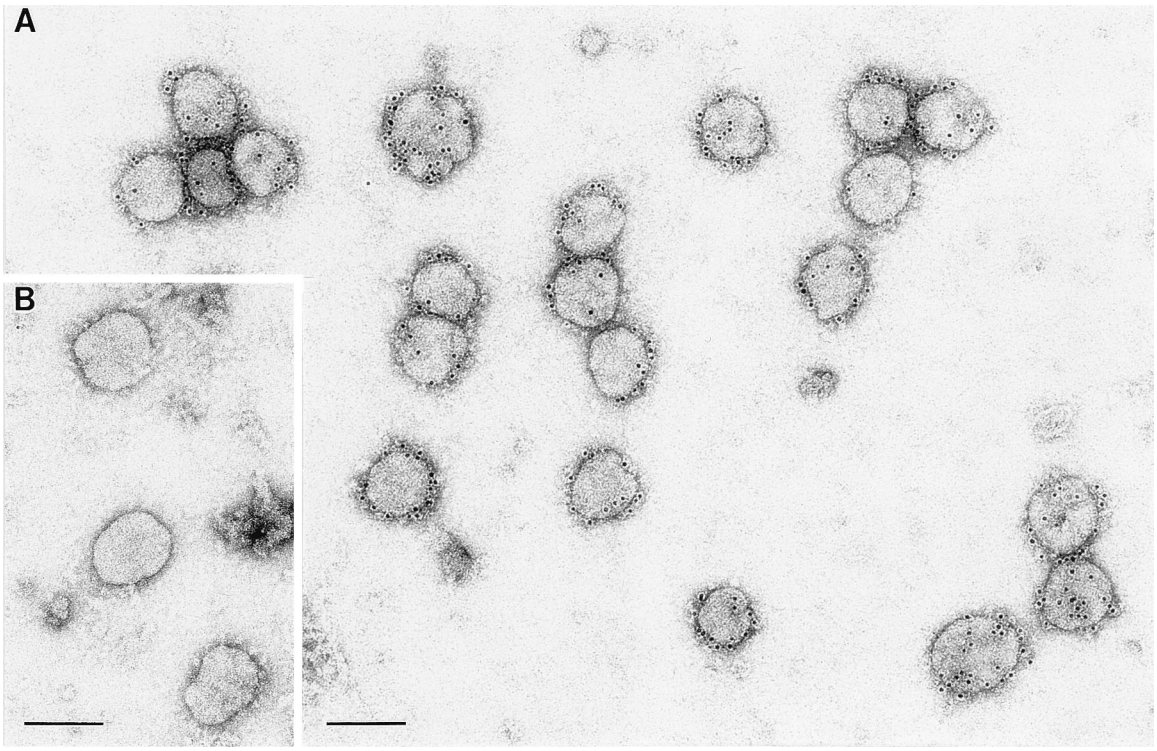

FIG. 4. Low-magnification fields of purified TGEV virions processed for the detection of the 9D.B4 site. (A) PUR46 virions are efficiently labeled with MAb 9D.B4 in the absence of nonspecific background. (B) MIL65 virions lacking the 9D.B4 site do not present any signal when incubated under the same conditions as for panel A. Bars, 100 nm.

Furthermore, labeling of PUR46 TGEV with 9D.B4 was not a marginal event, as this MAb labeled the virions with high efficiency (Fig. 4). Figure 4A presents a typical field showing both the highly specific labeling together with the absence of nonspecific background, while Fig. 4B shows MIL65 TGEV virions, which do not present any signal when incubated with 9D.B4 under the same conditions as used for PUR46 TGEV virions. Fixed PUR46 viruses, which have a more compact layer of spikes, still reacted with 9D.B4, although labeling was weaker (Fig. 3I), probably because of an impaired penetration of the antibodies through the layer of fixed spikes. In contrast, fixed MIL65 virions did not bind 9D.B4 (Fig. 3J). Another MAb that recognizes a different site of the carboxy-terminal region of M protein (3B.B3) also labeled the surface of PUR46 TGEV (Fig. 3K). 3B.B3 bound to MIL65 virions as well, although labeling was very weak (Fig. 3L). These data indicate that although the site for 3B.B3 is present in MIL65 TGEV, its accessibility to antibodies on the surface of the virus is less than for PUR46 virions. The loss of the epitope recognized by MAb 9D.B4 in MIL65 virions therefore seems to affect the topology and accessibility of other regions of M protein in the TGEV envelope. Detached envelopes derived from both PUR46 and MIL65 virions always exhibited a strong binding of MAb 3B.B3 (not shown). This finding confirms that the 3B.B3 site is present in both viral strains, although poorly exposed on the surface of intact MIL65 TGEV virions. A MAb (25.22) directed against an epitope of the amino-terminal region of M protein labels with similar patterns the surfaces of both PUR46 (Fig. 3M) and MIL65 (Fig. 3N) TGEV, providing a moderate signal intensity. Thus, this region of the protein seems to be exposed to similar extents in the two viral strains.

Topology of S and M proteins in virus-producing cell cultures. Preembedding immunogold labeling on cell cultures that are producing TGEV shows the proteins exposed either in outer cell membranes or on viral particles that have recently exited the infected cells. These nascent viruses were immunolabeled and fixed in situ, without previous manipulation. Viral particles are clearly identified at the intracellular level and outside the cells when visualized in Lowicryl sections of infected cells. The envelope of the extracellular virions is not precisely outlined in this embedding material, but the dense viral cores make viral particles very distinct from any cellular structure in Lowicryl ultrathin sections. Figure 5 shows the results obtained after preembedding labeling with different MAbs. MAb 9D.B4 labeled the virions released by PUR46 TGEV-producing cells (Fig. 5A), while it did not bind to MIL65 virions lacking this site (Fig. 5B). The decisive control of the MIL65 virions again confirms the specificity of immunodetection of the M protein C terminus in PUR46 TGEV virions. These results indicate that in PUR46 virions recently released from infected cells and not submitted to the manipulation of the purification procedure, the carboxy-terminal region of M protein is already exposed on the surface of the virions and accessible to antibodies. With MAb 6A.C3, a more intense labeling, associated with S protein, was obtained (Fig. 5C), while 3D.H10 (a MAb against the internal N protein) did not react with extracellular viruses (Fig. 5D), which confirms that the virus maintains its integrity under the conditions used in these experiments. The immunolabeling data described for TGEV virions are summarized in a quantitative analysis shown in Fig. 6. Clear differences between PUR46 and MIL65 TGEV strains were observed when the carboxy-terminal domain of M protein was detected (Fig. 6A, B, and E), while similar results were obtained for the two viral strains when S protein or the amino-terminal domain of M protein was labeled (Fig. 6C and D). S and M proteins were never detected free on the plasma

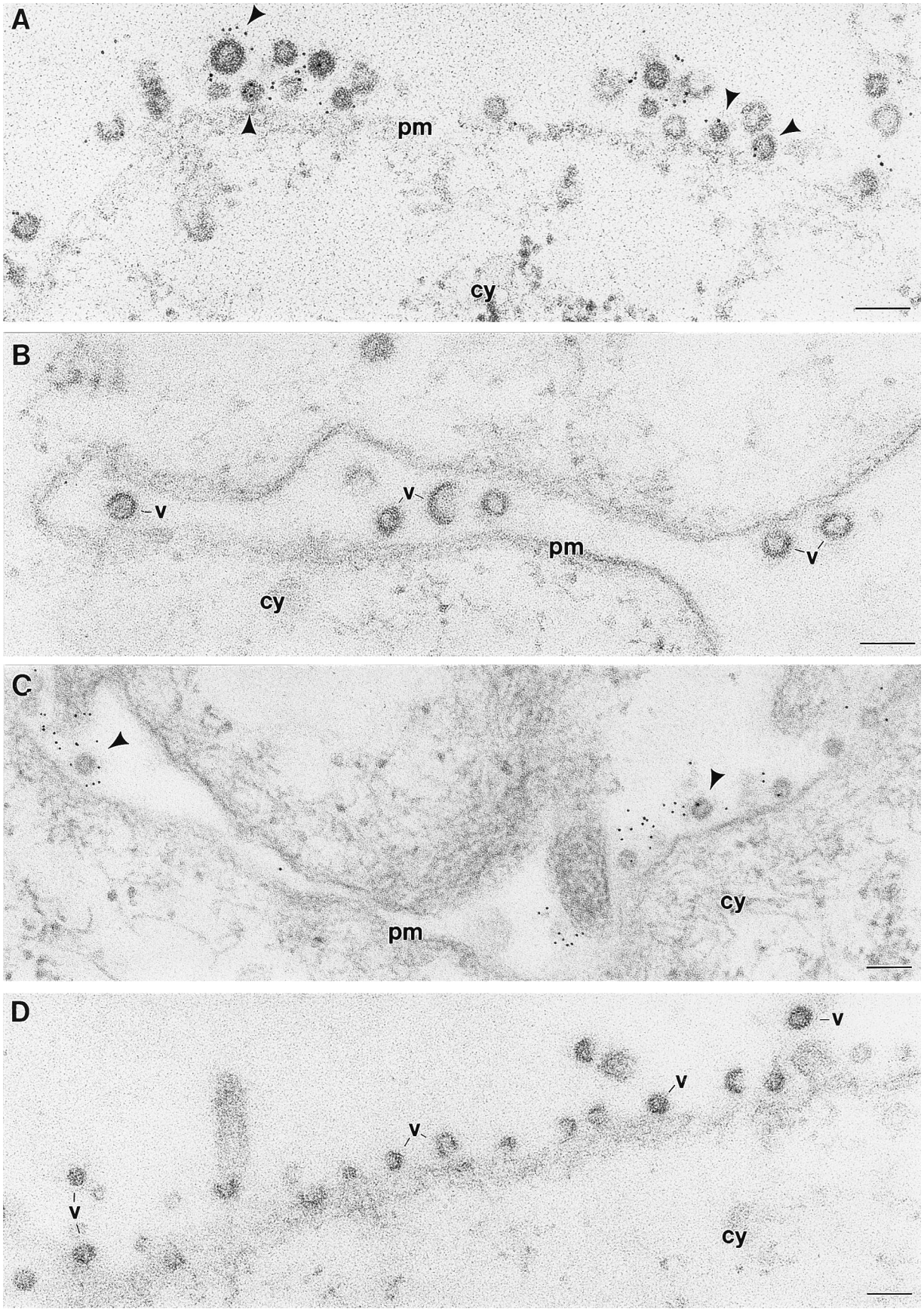
A
pm
cy
B
v
v
pm
v
cy
C
pm
cy
D
v
v
v
v
cy

FIG. 5. Preembedding immunogold labeling of TGEV proteins on virus-producing cultures. (A, C, and D) Cells infected with the PUR46 strain of TGEV; (B) a cell from a culture infected with the MIL65 strain. (A) MAb 9D.B4 added to the cultures labels the surface of PUR46 TGEV virions that recently exited the infected cells (arrowheads). (B) Extracellular MIL65 virions, which lack the 9D.B4 site, do not present any labeling. (C) Labeling with MAb 6A.C3 shows that the spike protein is also detected on virus particles adsorbed to the cell surface (arrowheads). (D) Cytochemical control with 3D.H10, a MAb directed against the internal nucleocapsid protein. When this MAb is used as the primary antibody, no labeling is obtained. pm, plasma membrane; cy, cytoplasm; v, extracellular virions. Bars, 100 nm.

membrane of ST cells at 14 h postinfection, and labeling associated to these proteins was always localized on viruses attached to the cell surface. The transport of TGEV glycoproteins to the cell surface has been previously detected at shorter postinfection times (22). If the early presence of these proteins on the plasma membrane of infected cells is not exclusively due to adsorbed viruses, our data suggest a transient transport of these proteins to the cell surface that would be maintained at very low levels or not at all late in infection.

TGEV neutralization by M-specific MAbs. PUR46-MAD and MIL65 strains of TGEV, harvested 20 h postinfection, were used for neutralization assays using S-, N-, and M-specific MAbs in the presence or absence of a rabbit antiserum against mouse immunoglobulins (Table 1). In previous neutralization studies, it was observed that diluting virus-antibody complexes before plating induces a significant decrease in the neutralization index, as a result of the reversibility of the neutralization reaction (41). As this was valid for all anti-TGEV MAbs tested, a small modification was introduced to increase the sensitivity of the neutralization assay described in previous works (14, 41) and to determine if M-specific antibodies could be weakly neutralizing. The assay was performed by incubating 10-fold dilutions of TGEV with the MAbs, and the mixtures were then plated on ST cells without further dilution. Under these conditions, two M-specific MAbs (9D.B4 and 3B.B3) neutralized the PUR46 strain (neutralization index, 0.5 to 0.9), the neutralization with MAb 3B.B3 being the most significant. In contrast, the MIL65 strain was not neutralized by these two MAbs (neutralization index, <0.3). The neutralization of PUR46 TGEV by MAb 3B.B3 was similar to that observed with MAb 25.22, which is specific for the amino terminus of M protein. Background neutralization by MAbs and standard deviations were always below 0.3 logarithmic units. These data indicate that up to 87% of the viral infectivity could be neutralized by a MAb that binds to the carboxy-terminal domain of M protein. Neutralization by MAbs specific for the M protein carboxy terminus did not increase with the presence of a second antibody or complement, but it did in the case of the MAb against the amino terminus of M protein or for S-specific MAbs 8F.B3 and 1D.G3 (Table 1).

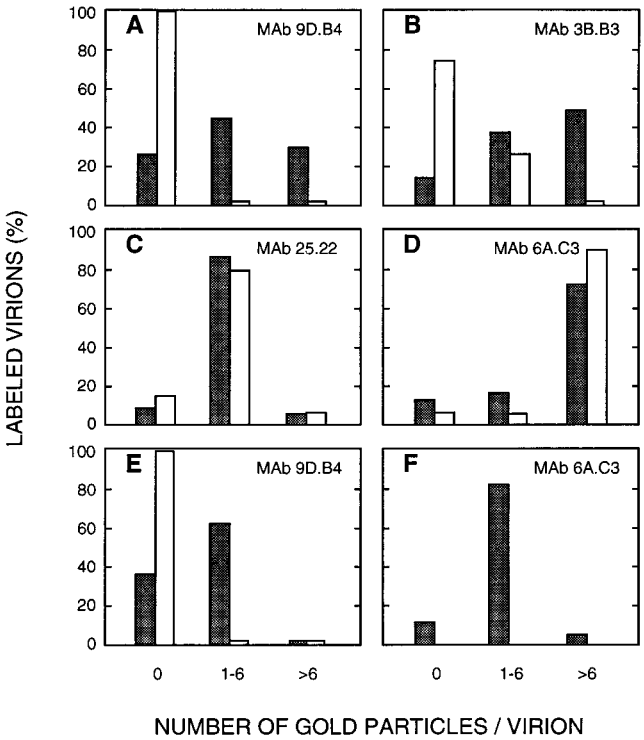

FIG. 6. Quantitative analysis of the immunogold labeling of M and S proteins on TGEV virions. (A to D) Results corresponding to labeling of purified viruses; (E and F) results obtained with nascent virions associated with the surface of infected cells and labeled in situ by a preembedding procedure. Filled bars correspond to PUR46 TGEV, and open bars show the results obtained for MIL65 TGEV. The percentage of virions with zero, one to six, and more than six gold particles per virion is shown for each MAb. Clear differences between the two viral strains are observed when the C terminus of M protein is localized (MAbs 9D.B4 and 3B.B3) (see text). However, the results are similar for the two viral strains when the amino terminus of M protein (MAb 25.22) or S protein (MAb 6A.C3) is detected. One hundred purified virions were counted for each MAb and viral strain (A to D). In preembedding labeling experiments (E, F), an average of 250 nascent virions on the surface of infected cells were counted for each MAb and viral strain.

DISCUSSION

The protein domains exposed on the surface of viruses play fundamental roles in infection, by binding to cell receptors, promoting cell fusion processes, or interacting with elements of the host immune system. Hence, analysis of viral architecture and assembly and of the topology of surface proteins is important for defining the main events of the viral life cycle.

The membrane (M) glycoprotein of coronaviruses seems to

TABLE 1. Neutralization of TGEV with MAbs specific for structural proteins

Specificity	MAb	Neutralization index for[a]:			
		PUR46		MIL65	
		−2nd antibody	+2nd antibody	−2nd antibody	+2nd antibody
S	8F.B3	0.5	1.0	ND	ND
	1D.G3	0.6	2.0	ND	ND
N	3D.H10	<0.3	<0.3	<0.3	<0.3
	3C.D8	<0.3	<0.3	<0.3	<0.3
M	3B.B3	0.9	0.8	<0.3	<0.3
	9D.B4	0.5	0.6	<0.3	<0.3
	3D.E3	0.4	0.3	<0.3	<0.3
	3B.D3	0.4	0.4	<0.3	<0.3
	25.22	0.8	1.5	ND	ND

[a] Tenfold dilution aliquots of TGEV were neutralized with 1 volume of undiluted hybridoma supernatant containing the indicated MAb. Then 1 volume of a 20-fold dilution of rabbit anti-mouse immunoglobulins was added, and the mixture was further incubated as indicated in Materials and Methods. The number of PFU of virus per milliliter mixed with normal medium was divided by the number of PFU of virus per milliliter in the presence of a given MAb, and the neutralization index was expressed as the $\log_{10}$ of this ratio. ND, not determined.

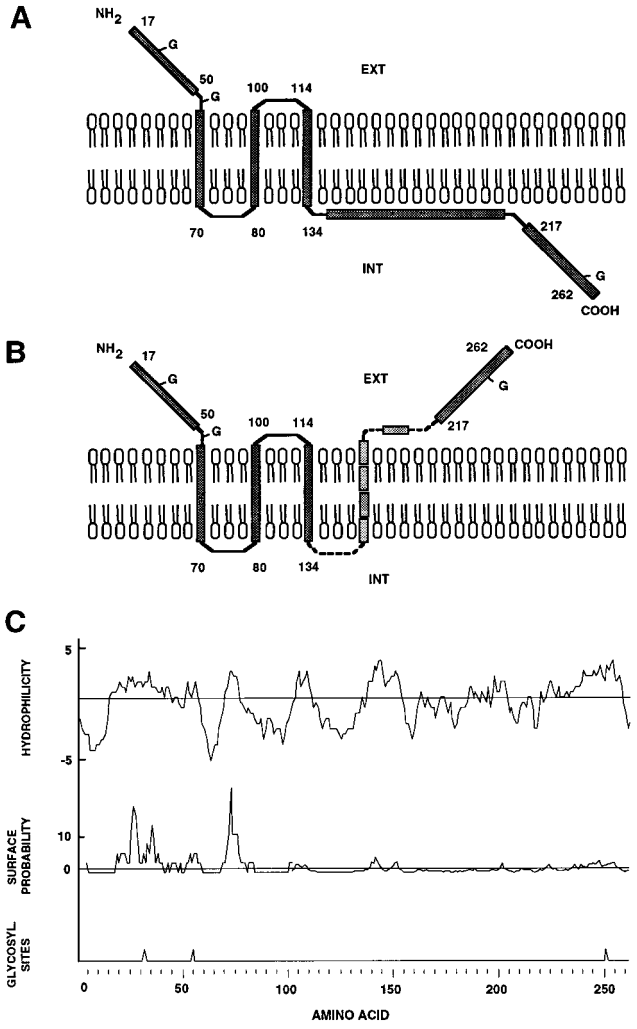

FIG. 7. Topology and structural features of the membrane protein of TGEV. (A) Topological model originally proposed for the M protein of coronaviruses. EXT, exterior; INT, interior. (B) Alternative model inferred from the results discussed in this report and proposed for the membrane protein of TGEV. Both topologies probably coexist in TGEV virions. (C) Hydrophilicity, surface probability, and glycosylation site profiles of TGEV M protein as determined with the computer programs developed by Devereux et al. (9).

be involved in viral morphogenesis. Intracellular interactions of M protein with the small membrane protein (sM), the spike (S) glycoprotein, and the viral nucleocapsid have been proposed as essential for virus assembly (13, 38, 43). Although previous studies with MHV and IBV M proteins support the topological model shown in Fig. 7A, experimental evidence supports the view that at least in the case of TGEV, M protein molecules with the currently accepted topology could coexist with a significant number of molecules exhibiting an alternative topology. The carboxy terminus of TGEV M protein has been localized by immunofluorescence and by antibody-mediated complement-dependent cytolysis on the surface of TGEV-infected ST cells (10, 22). These data indicate that in TGEV-infected cells, at least some of the M molecules have the carboxy terminus exposed toward the extracellular environment. Our immunolabeling mapping of TGEV M protein clearly detects both the amino and carboxy termini of the protein exposed on the surface of purified viruses, as well as in native, nonmanipulated virions that recently exited the cells and were labeled in situ. This alternative topology is present in the functional virus, since its infectivity is neutralized by MAbs against the exposed C terminus of M protein. All of this experimental evidence is in agreement with the topology of the M protein proposed in Fig. 7B. To firmly establish that the carboxy terminus of M protein is exposed on the virus surface, it has to be ruled out that our results could be due to nonspecific binding of the antibodies, to free M protein adsorbed to the virion surface, or to lack of virion integrity. These potential artifacts have been discarded since the carboxy-terminus-specific MAb 9D.B4 did not bind the MIL65 strain of TGEV, the carboxy-terminus-specific MAbs 3B.D3 and 3D.E3 did not bind TGEV particles, and the TGEV virions did not bind MAbs specific for the internal N protein.

Indirect evidences also support the proposed alternative topology. Analysis of the M protein hydrophilicity pattern shows three highly hydrophobic domains, which span the membrane three times (2, 16, 19, 31, 33). Hydrophilicity, exposure, and flexibility profiles of M protein show a fourth segment in TGEV M protein (from amino acids 155 to 185) that has low hydrophilicity and low probability of surface exposure (Fig. 7C). By contrast, the final 46 amino acids are mostly hydrophilic and have a high probability of being exposed on the surface. These data are compatible with a potential fourth spanning domain, a possibility that cannot be discarded from the model proposed by Armstrong et al. (1). Since the hydrophobicity of the fourth segment is not very high, probably only part of the population of TGEV M molecules expose their carboxy termini. This domain of M protein, interestingly, happens to be antigenically dominant both in MHV (42) and TGEV, as shown in this report. In addition, the M protein carboxy-terminal domain has a potential glycosylation site (Fig. 7C) in some viral isolates (3, 21), and these sites are preferentially located in exposed areas of the proteins. The evidence obtained for the alternative topology of TGEV M protein is not in conflict with the organization of the molecule proposed previously for the MHV M protein (1). In fact, a number of the M molecules could exhibit the conventional organization, while another population could be in the alternative topology, as observed for mutant M proteins of MHV (24). Interestingly, although the amino acid sequences of TGEV and MHV M proteins exhibit only 32% homology (16), the corresponding theoretical hydrophilicity plots of the two proteins are very similar. This finding suggests that the alternative topology proposed for TGEV M protein might also be present in MHV virions. Further studies will be necessary to confirm this possibility.

Even if the exposure of the M protein carboxy terminus is a consequence of late topological changes during viral morphogenesis, it is important to note that this protein domain is finally exposed in the infective extracellular TGEV virions. The exposure of this domain has functional relevance, since TGEV-infected cells are lysed by MAbs specific for the carboxy terminus, and the infectious virus is neutralized by these MAbs. Whether this topology of the membrane protein is shared by other coronaviruses or is exclusive to TGEV is unresolved.

ACKNOWLEDGMENTS

This work was supported by grants from the Consejo Superior de Investigaciones Científicas, the Comisión Interministerial de Ciencia y Tecnología, and the Consejería de Educación y Cultura de la Comunidad de Madrid from Spain and by the European Communities (projects "Science" and "Biotech"). Fellowships from the Spanish Ministry of Education and Science (I.M.A. and C.S.) are also acknowledged.

REFERENCES

1. **Armstrong, J., H. Niemann, S. Smeekens, P. Rottier, and G. Warren.** 1984. Sequence and topology of a model intracellular membrane protein, E1 glycoprotein, from a coronavirus. Nature (London) **308:**751–752.
2. **Boursnell, M. E. G., T. D. K. Brown, and M. M. Binns.** 1984. Sequence of the membrane protein gene from avian coronavirus IBV. Virus Res. **1:**303–313.
3. **Britton, P., R. S. Carmenes, K. W. Page, and D. J. Garwes.** 1988. The integral membrane protein from a virulent isolate of transmissible gastroenteritis virus. Mol. Microbiol. **2:**497–505.
4. **Burnette, W. N.** 1981. Western-blotting: electrophoretic transfer from sodium dodecyl sulfate-polyacrylamide gels to unmodified nitrocellulose and radiographic detection with radioiodinated protein A. Anal. Biochem. **112:** 195–203.
5. **Carrascosa, J. L.** 1988. Immunoelectron microscopical studies on viruses. Electron Microsc. Rev. **1:**1–16.
6. **Correa, I., and L. Enjuanes.** Unpublished data.
7. **Correa, I., G. Jiménez, C. Suñé, M. J. Bullido, and L. Enjuanes.** 1988. Antigenic structure of the E2 glycoprotein from transmissible gastroenteritis coronavirus. Virus Res. **10:**77–94.
8. **Delmas, B., J. Gelfi, and H. Laude.** 1986. Antigenic structure of transmissible gastroenteritis virus. II. Domains in the peplomer glycoprotein. J. Gen. Virol. **67:**1405–1418.
9. **Devereux, J., P. Haeberli, and O. Smithies.** 1984. A comprehensive set of sequence analysis programs for VAX. Nucleic Acids Res. **12:**387–395.
10. **Enjuanes, L.** Unpublished data.
11. **Gebauer, F., W. A. P. Posthumus, I. Correa, C. Suñé, C. M. Sánchez, C. Smerdou, J. A. Lenstra, R. Meloen, and L. Enjuanes.** 1991. Residues involved in the formation of the antigenic sites of the S protein of transmissible gastroenteritis coronavirus. Virology **183:**225–238.
12. **Godet, M., R. L'Haridon, J. F. Vautherot, and H. Laude.** 1992. TGEV coronavirus ORF4 encodes a membrane protein that is incorporated into virions. Virology **188:**666–675.
13. **Griffiths, G., and P. J. M. Rottier.** 1992. Cell biology of viruses that assemble along the biosynthetic pathway. Semin. Cell Biol. **3:**367–381.
14. **Jiménez, G., I. Correa, M. P. Melgosa, M. J. Bullido, and L. Enjuanes.** 1986. Critical epitopes in transmissible gastroenteritis virus neutralization. J. Virol. **60:**131–139.
15. **Kapke, P. A., and D. A. Brian.** 1986. Sequence analysis of the porcine transmissible gastroenteritis coronavirus nucleocapsid protein gene. Virology **151:**41–49.
16. **Kapke, P. A., F. Y. T. Tung, B. G. Hogue, D. A. Brian, R. D. Woods, and R. Wesley.** 1988. The amino-terminal signal peptide on the porcine transmissible gastroenteritis coronavirus matrix protein is not an absolute requirement for membrane translocation and glycosylation. Virology **165:**367–376.
17. **Kellenberger, E., and M. A. Hayat.** 1991. Some basic concepts for the choice of methods, p. 1–30. *In* M. A. Hayat (ed.), Colloidal gold. Principles, methods, and applications. Academic Press, London.
18. **Laemmli, U. K.** 1970. Cleavage of structural proteins during the assembly of the head of bacteriophage T4. Nature (London) **227:**680–685.
19. **Lapps, W., B. G. Hogue, and D. A. Brian.** 1987. Sequence analysis of the bovine coronavirus nucleocapsid and matrix protein genes. Virology **157:**47–57.
20. **Laude, H., J. M. Chapsal, J. Gelfi, S. Labiau, and J. Grosclaude.** 1986. Antigenic structure of transmissible gastroenteritis virus. I. Properties of monoclonal antibodies directed against virion proteins. J. Gen. Virol. **67:** 119–130.
21. **Laude, H., D. Rasschaert, and J. C. Huet.** 1987. Sequence and N-terminal processing of the transmembrane protein E1 of the coronavirus transmissible gastroenteritis virus. J. Gen. Virol. **68:**1687–1693.
22. **Laviada, M. D., S. P. Videgain, L. Moreno, F. Alonso, L. Enjuanes, and J. M. Escribano.** 1990. Expression of swine transmissible gastroenteritis virus envelope antigens on the surface of infected cells: epitopes externally exposed. Virus Res. **16:**247–254.
23. **Locker, J. K., J. Klumperman, V. Oorschot, M. C. Horzinek, H. J. Geuze, and P. J. M. Rottier.** 1994. The cytoplasmic tail of mouse hepatitis virus M protein is essential but not sufficient for its retention in the Golgi complex. J. Biol. Chem. **269:**28263–28269.
24. **Locker, J. K., J. K. Rose, M. C. Horzinek, and P. J. M. Rottier.** 1992. Membrane assembly of the triple-spanning coronavirus M protein. J. Biol. Chem. **267:**21911–21918.
25. **McClurkin, A. W., and J. O. Norman.** 1966. Studies on transmissible gastroenteritis of swine. II. Selected characteristics of a cytopathogenic virus common to five isolates from transmissible gastroenteritis. Can. J. Comp. Vet. Sci. **30:**190–198.
26. **Menéndez-Arias, L., C. Risco, P. Pinto da Silva, and S. Oroszlan.** 1992. Purification of immature cores of mouse mammary tumor virus and immunolocalization of protein domains. J. Virol. **66:**5615–5620.
27. **Rasschaert, D., and H. Laude.** 1987. The predicted primary structure of the peplomer protein E2 of the porcine coronavirus transmissible gastroenteritis virus. J. Gen. Virol. **68:**1883–1890.
28. **Risco, C., J. L. Carrascosa, and M. A. Bosch.** 1991. Uptake and subcellular distribution of *Escherichia coli* lipopolysaccharide by isolated rat type II pneumocytes. J. Histochem. Cytochem. **39:**607–615.
29. **Risco, C., L. Menéndez-Arias, T. D. Copeland, P. Pinto da Silva, and S. Oroszlan.** J. Cell Sci., in press.
30. **Risco, C., and P. Pinto da Silva.** 1995. Cellular functions during activation and damage by pathogens: immunogold studies of the interaction of bacterial endotoxins with target cells. Microsc. Res. Tech. **31:**141–158.
31. **Rottier, P., D. Brandenburg, J. Armstrong, B. A. M. Van der Zeijst, and G. Warren.** 1984. Assembly in vitro of a spanning membrane protein of the endoplasmic reticulum: the E1 glycoprotein of coronavirus mouse hepatitis virus A59. Proc. Natl. Acad. Sci. USA **81:**1421–1425.
32. **Rottier, P. J., M. C. Horzinek, and B. A. M. Van der Zeijst.** 1981. Viral protein synthesis in mouse hepatitis virus strain A59-infected cells: effect of tunicamycin. J. Virol. **40:**350–357.
33. **Rottier, P. J., G. W. Welling, S. Welling-Wester, H. G. Niesters, J. A. Lenstra, and B. A. M. Van der Ziejst.** 1986. Predicted membrane topology of the coronavirus protein E1. Biochemistry **25:**1335–1339.
34. **Ruther, U., and B. Muller-Hill.** 1983. Easy identification of cDNA clones. EMBO J. **2:**1791–1794.
35. **Sachs, D., G. Leight, J. Cone, S. Schwarz, L. Stuart, and S. Rosemberg.** 1976. Transplantation in miniature swine. I. Fixation of the major histocompatibility complex. Transplantation **22:**559–567.
36. **Saif, L. J., and R. D. Wesley.** 1992. Transmissible gastroenteritis, p. 362–386. *In* A. D. Leman, B. Straw, W. L. Mengeling, S. D'Allaire, and D. J. Taylor (ed.), Diseases of swine. Iowa State University Press, Ames.
37. **Sánchez, C. M., G. Jiménez, M. D. Laviada, I. Correa, C. Suñé, M. J. Bullido, F. Gebauer, C. Smerdou, P. Callebaut, J. M. Escribano, and L. Enjuanes.** 1990. Antigenic homology among coronaviruses related to transmissible gastroenteritis virus. Virology **174:**410–417.
38. **Spaan, W., G. Cavanagh, and H. C. Horzinek.** 1988. Coronaviruses: structure and genome expression. J. Gen. Virol. **69:**2939–2952.
39. **Sturman, L., and K. Holmes.** 1985. The novel glycoproteins of coronaviruses. Trends Biochem. Sci. **10:**17–20.
40. **Sturman, L. S.** 1981. The structure and behavior of coronavirus A59 glycoproteins. Adv. Exp. Med. Biol. **142:**1–18.
41. **Suñé, C., G. Jiménez, I. Correa, M. J. Bullido, F. Gebauer, C. Smerdou, and L. Enjuanes.** 1990. Mechanisms of transmissible gastroenteritis coronavirus neutralization. Virology **177:**559–569.
42. **Tooze, S. A., and K. K. Stanley.** 1986. Identification of two epitopes in the carboxy-terminal 15 amino acids of the E1 glycoprotein of mouse hepatitis virus A59 by using hybrid proteins. J. Virol. **60:**928–934.
43. **Vennema, H., G.-J. Godeke, M. C. Horzinek, and P. J. M. Rottier.** 1994. Assembly of coronavirus-like particles from co-expressed structural protein genes, p. 135. *In* Abstracts of the VIth International Symposium on Corona and Related Viruses 1994. Québec, Ontario, Canada.
44. **Woods, R. D., R. Wesley, and P. A. Kapke.** 1987. Complement-dependent neutralization of transmissible gastroenteritis virus by monoclonal antibodies. Adv. Exp. Med. Biol. **218:**493–500.